August 2010

A comprehensive analysis of the dark matter direct detection experiments in the mirror dark matter framework

R. Foot[1]

School of Physics,
University of Melbourne,
Victoria 3010 Australia

Mirror dark matter offers a framework to explain the existing dark matter direct detection experiments. Here we confront this theory with the most recent experimental data, paying attention to the various known systematic uncertainties, in quenching factor, detector resolution, galactic rotational velocity and velocity dispersion. We perform a detailed analysis of the DAMA and CoGeNT experiments assuming a negligible channeling fraction and find that the data can be fully explained within the mirror dark matter framework. We also show that the mirror dark matter candidate can explain recent data from the CDMS/Ge, EdelweissII and CRESSTII experiments and we point out ways in which the theory can be further tested in the near future.

[1]E-mail address: rfoot@unimelb.edu.au

1 Introduction

The field of dark matter direct detection has blossomed in recent times, with exciting positive signals from DAMA[1, 2, 3], CoGeNT[4], as well as interesting hints from CDMS/Ge[5] and CDMS electron scattering[6]. Very recently, more exciting evidence for the direct detection of dark matter has arisen from the CRESSTII[7] and EdelweissII[8] experiments.

Mirror dark matter has emerged as a simple predictive framework which can explain all of the direct detection experiments[9, 10, 11, 12, 13]. The purpose of this article is to provide a comprehensive update of the experimental status of the mirror dark matter candidate, paying particular attention to the various known systematic uncertainties,in quenching factor, detector resolution, galactic rotational velocity and velocity dispersion.

Recall, mirror dark matter posits that the inferred dark matter in the Universe arises from a hidden sector which is an exact copy of the standard model sector[14] (for a review see ref.[15]). That is, a spectrum of dark matter particles of known masses are predicted: $e', H', He', O', Fe', ...$ (with $m_{e'} = m_e, m_{H'} = m_H$, etc). The galactic halo is then presumed to be composed predominately of a spherically distributed self interacting mirror particle plasma comprising these particles[16]. In addition to gravity, ordinary and mirror particles interact with each other via (renormalizable) photon-mirror photon kinetic mixing[14, 17]:

$$\mathcal{L}_{mix} = \frac{\epsilon}{2} F^{\mu\nu} F'_{\mu\nu} \ , \tag{1}$$

where $F_{\mu\nu}$ ($F'_{\mu\nu}$) is the ordinary (mirror) $U(1)$ gauge boson field strength tensor. This interaction enables mirror charged particles to couple to ordinary photons with electric charge $q = \epsilon e$ and thus allows mirror particles to elastically scatter off ordinary particles. This means that mirror dark matter can be probed in dark matter direct detection experiments. It turns out that this simple predictive theory can explain the DAMA annual modulation signal, the CoGeNT low energy excess as well as hints from CDMS, Edelweiss and CRESSTII consistently with the null results of other experiments.

The outline of this paper is as follows. In section 2 we provide a brief review of the mirror dark matter theory. In section 3 we provide some necessary technical details: cross section and halo distribution which are characteristic of mirror dark matter. In section 4 (5), we examine the implications of the most recent DAMA (CoGeNT) data for the mirror dark matter theory. These experiments are sensitive to dark matter particles heavier than around 10 GeV which makes them excellent probes of the dominant mirror metal component of the galactic halo, A'. We show that these experiments can be simultaneously explained and lead to a measurement of the parameters: $\epsilon\sqrt{\xi_{A'}}$ and $m_{A'}$ both of which are consistent with the theoretical expectations of $\epsilon \sim 10^{-9}$ (from galactic halo energy balance) and $A' \sim O' \Rightarrow m_{A'} \sim 16 m_p$ (from analogy with the ordinary matter sector). In section 5 we also show that the DAMA and CoGeNT signals are consistent with the results of the other

experiments including the null results of XENON100 and CDMS/Si. In section 6 we examine the constraints on e' scattering from the DAMA absolute rate. We show that these constraints when combined with the DAMA and CoGeNT data suggest a halo mirror metal proportion $\xi_{A'} \gtrsim 10^{-2}$. In section 7 we examine recent data from the CDMS/Ge, EdelweissII and CRESSTII experiments. CDMS/Ge and Edelweiss are excellent probes of the anticipated Fe' component, and the data are consistent with a Fe' component with mass fraction: $\xi_{Fe'}/\xi_{A'} \sim 10^{-2}$. We also point out that the CRESSTII experiment is potentially sensitive to both A' and Fe' components and their recently announced low energy excess can be explained by A' and Fe' interactions. In section 8 we draw our conclusions.

2 A brief review of mirror dark matter

Mirror dark matter conjectures that the inferred dark matter in the Universe arises from a hidden sector which is an exact copy of the standard model sector. That is, the standard model of particle physics is extended:

$$\mathcal{L} = \mathcal{L}_{SM}(e, u, d, \gamma, ...) + \mathcal{L}_{SM}(e', u', d', \gamma', ...) \ . \tag{2}$$

Such a theory can be theoretically well motivated from symmetry considerations if left and right handed chiral fields are interchanged in the extra sector. In this way space-time parity symmetry and in fact the full Poincaré group can be realized as an unbroken symmetry of nature, and for this reason we refer to the particles in the extra sector as mirror particles. The standard model extended with a mirror sector was first studied in ref.[14] and shown to be a phenomenologically consistent renormalizable extension of the standard model. The concept, though, has a long history dating back prior to the advent of the standard model of particle interactions[18]. For a review and more complete list of references see ref.[15].

If we include all interaction terms consistent with renormalizability and the symmetries of the theory then we must add to the Lagrangian a $U(1)$ kinetic mixing interaction[17, 14] and Higgs - mirror Higgs quartic coupling[14]:

$$\mathcal{L}_{mix} = \frac{\epsilon}{2} F^{\mu\nu} F'_{\mu\nu} + \lambda \phi^\dagger \phi \phi'^\dagger \phi' \ , \tag{3}$$

where $F_{\mu\nu}$ ($F'_{\mu\nu}$) is the ordinary (mirror) $U(1)$ gauge boson field strength tensor and ϕ (ϕ') is the electroweak Higgs (mirror Higgs) field. The most general Higgs potential, including the quartic Higgs mixing term (above) was studied in ref.[14] and shown to have the vacuum $\langle \phi \rangle = \langle \phi' \rangle$ for a large range of parameters. With this vacuum, the mirror symmetry is unbroken and consequently the masses of the mirror particles are all identical to their ordinary matter counterparts.

In this framework, dark matter is comprised of a spectrum of stable massive mirror particles: $e', H', He', O'...$ etc, with masses $m_{e'} = m_e, m_{H'} = m_H$, $m_{He'} = m_{He}$ etc. To explain the rotation curves in spiral galaxies, the dark matter needs to be roughly spherically distributed in galactic halos. Given the upper limit on

compact star sized objects (MACHOs) in the halo from microlensing observations, roughly $f_{macho} \lesssim 0.2 - 0.3$ depending on the assumptions[19], we then expect the mirror particles to be distributed predominately as a hot gaseous spherical halo surrounding the collapsed disk of ordinary matter[16] [2].

Observations of colliding clusters, such as the bullet cluster[20] indicate that dark matter does not have self interactions on galaxy cluster scales. This suggests that the gaseous mirror dark matter component is confined to galactic halos (c.f. [21]). Gravity and the mirror particle self interactions may well be sufficient to achieve this.

A dissipative dark matter candidate like mirror matter can only survive in an extended spherical distribution in galaxies without collapsing if there is a substantial heating mechanism to replace the energy lost due to radiative cooling. In fact, ordinary supernova can plausibly supply the required heating if the photon and mirror photon are kinetically mixed with $\epsilon \sim 10^{-9}$[16] [3]. For kinetic mixing of this magnitude about half of the total energy emitted in ordinary Type II Supernova explosions ($\sim 3 \times 10^{53}$ erg) will be in the form of light mirror particles ($\nu'_{e,\mu,\tau}$, $e'^{\pm}$, γ') originating from kinetic mixing induced plasmon decay into $e'^{+}e'^{-}$ in the supernova core[23]. Given the observed rate of Supernova's in our galaxy of about 1 per century, this implies a heating of the halo (principally due to the $e'^{\pm}$ component), of around:

$$L^{SN}_{heat-in} \sim \frac{1}{2} \times 3 \times 10^{53}\ erg \frac{1}{100\ years} \sim 10^{44}\ \text{erg/s, for the Milky Way .} \qquad (4)$$

It turns out that this matches (to within uncertainties) the energy lost from the halo due to radiative cooling[16]:

$$L^{halo}_{energy-out} = \Lambda \int n^2_{e'} 4\pi r^2 dr \sim 10^{44}\ \text{erg/s, for the Milky Way.} \qquad (5)$$

In other words, a gaseous mirror particle halo can potentially survive without collapsing because the energy lost due to dissipative interactions can be replaced by the energy from ordinary supernova explosions. Presumably there are feedback mechanisms which maintain this balance. For example if $L^{halo}_{energy-out} > L^{SN}_{heat-in}$ then the halo would contract which in turns increases the gravitational pull on the ordinary matter component. This compression of the ordinary matter component should increase ordinary star formation rates, thereby increasing $L^{SN}_{heat-in}$ until the energy is balanced. In this way the ordinary supernova rate might be dynamically adjusted so that the halo is stabilized. Extending these ideas to galaxies beyond the Milky Way, the hypothesized connection between Supernova rates and dark matter distribution

[2]Naturally a MACHO subcomponent consisting of mirror white dwarfs, mirror neutron stars etc are also expected and can be probed by microlensing observations. Since most of the stellar mass is ejected as gas in the explosions producing these stellar remnants, it is plausible that the MACHO mass fraction can satisfy the observational limit of $f_{macho} \lesssim 0.2 - 0.3$.

[3]A mirror sector with such kinetic mixing is consistent with all known laboratory, astrophysical and cosmological constraints[22].

might ultimately provide a dynamical justification for the empirical Tully-Fischer and Faber-Jackson relations.

The spherically distributed mirror particle plasma is likely to be far too hot for much mirror star formation to occur at the present epoch. Thus, we do not expect significant heating of the ordinary matter sector from mirror Supernovas at the present time. However during the first billion years or so the situation might have been the reverse. That is, the early stages of galaxies may have witnessed rapid mirror star formation and evolution and little ordinary star formation, due ultimately to the effects of asymmetric initial conditions in the Early Universe. In particular, for $T' \ll T$ in the early Universe (required to achieve successful big bang nucleosynthesis and large scale structure formation)[4] and $\epsilon \sim 10^{-9}$ the primordial mirror He' abundance is expected to be relatively high, $Y_{He'} \approx 0.9$[24]. With such initial conditions the evolution rate of stars is dramatically increased by several orders of magnitude[25]. In other words, we surmise that the required asymmetric evolution of the ordinary and mirror matter components in galaxies, originates in the complex interactions between the ordinary and mirror components (such as the energy transfer to the mirror sector from ordinary supernova's) together with asymmetric initial conditions in the early Universe.

Since mirror charged particles have an electric charge induced via the kinetic mixing, mirror nuclei can interact with ordinary nuclei via spin independent Rutherford elastic scattering. It turns out that the positive results of DAMA and CoGeNT can be explained by such scattering from a putative $\sim O'$ component if $\epsilon \sim 10^{-9}$. This provides important experimental evidence in favour of the mirror dark matter candidate, which we now examine in detail.

3 Interaction cross-section and galactic mirror dark matter distribution

The interaction rate in an experiment depends on the cross-section, $d\sigma/dE_R$, and halo velocity distribution, $f(v)$. The photon-mirror photon kinetic mixing enables a mirror nucleus [with mass and atomic numbers A', Z' and velocity v] to elastically scatter with an ordinary nucleus [presumed at rest with mass and atomic numbers A, Z]. In fact the cross-section is just of the standard Rutherford form corresponding to a particle of electric charge Ze scattering off a particle of electric charge $\epsilon Z'e$. The cross-section can be expressed in terms of the recoil energy of the ordinary nucleus, E_R[9]:

$$\frac{d\sigma}{dE_R} = \frac{\lambda}{E_R^2 v^2} \ , \tag{6}$$

[4]See ref.[26] for further discussions about early Universe cosmology with mirror dark matter.

where

$$\lambda \equiv \frac{2\pi\epsilon^2 Z^2 Z'^2 \alpha^2}{m_A} F_A^2(qr_A) F_{A'}^2(qr_{A'}) \ , \tag{7}$$

and $F_X(qr_X)$ $(X = A, A')$ are the form factors which take into account the finite size of the nuclei and mirror nuclei. [The quantity $q = (2m_A E_R)^{1/2}$ is the momentum transfer and r_X is the effective nuclear radius][5]. A simple analytic expression for the form factor, which we adopt in our numerical work, is the one given by Helm[27, 28]:

$$F_X(qr_X) = 3\frac{j_1(qr_X)}{qr_X} e^{-(qs)^2/2} \ , \tag{8}$$

with $r_X = 1.14X^{1/3}$ fm, $s = 0.9$ fm and j_1 is the spherical Bessel function of index 1.

The halo mirror particles are presumed to form a self interacting plasma at an isothermal temperature T. This means that the halo distribution function is given by a Maxwellian distribution:

$$\begin{aligned} f_i(v) &= e^{-\frac{1}{2}m_i v^2/T} \\ &= e^{-v^2/v_0^2[i]} \ , \end{aligned} \tag{9}$$

where the index i labels the particle type $[i = e', H', He', O', Fe', ...]$ and $v_0^2[i] \equiv 2T/m_i$. The dynamics of such a mirror particle plasma has been investigated previously[16, 9], where it was found that the condition of hydrostatic equilibrium implied that the temperature of the plasma satisfied:

$$T \simeq \frac{1}{2}\bar{m} v_{rot}^2 \ , \tag{10}$$

where $\bar{m} = \sum n_i m_i / \sum n_i$ is the mean mass of the particles in the plasma, and $v_{rot} \approx 254 \pm 16$ km/s is the galactic rotational velocity of the Milky Way[29]. The velocity dispersion of the particles in the mirror particle halo evidently depends on the particular particle species and satisfies:

$$v_0^2[i] = v_{rot}^2 \frac{\overline{m}}{m_i} \ . \tag{11}$$

Note that if $m_i \gg \overline{m}$, then $v_0^2[i] \ll v_{rot}^2$. Consequently heavy mirror nuclei have their velocities (and hence energies) relative to the Earth boosted by the Earth's (mean) rotational velocity around the galactic center, $\approx v_{rot}$. This allows a mirror nuclei in the 'oxygen' mass range $\sim m_0 \approx 15$ GeV to provide a significant annual modulation signal in the energy region probed by DAMA ($E_R > 2$ keVee) which, as we will see, has the right properties to fully account for the data presented by the DAMA collaboration[1, 2, 3].

[5]Unless otherwise specified, we use natural units, $\hbar = c = 1$ throughout.

According to the above considerations, in order to calculate the velocity dispersion, $v_0^2[i]$, we need to estimate the mean mass of the mirror particles in the plasma. The plasma is expected to be completely ionized since it turns out that the temperature of the plasma is $T \approx \frac{1}{2}$ keV. We start by making the simplifying assumption that the mirror metal component of the plasma is dominated by a single element, A'. Under this assumption, the plasma consists of e', H', He' and A'. It is straightforward to estimate $\bar{m}$:

$$\frac{\bar{m}}{m_p} \simeq \frac{1}{2 - \frac{5}{4}\xi_{He'} + \xi_{A'}(\frac{1}{A'} - \frac{3}{2})} \ , \tag{12}$$

where $\xi_i \equiv \frac{n_i m_i}{n_{H'} m_p + n_{He'} m_{He} + n_{A'} m_{A'}}$ is the halo mass fraction of species i, m_p is the proton mass and A' is the mass number. Thus, combining Eq.(11) and Eq.(12) we have

$$v_0^2[A'] = \frac{v_{rot}^2}{A'[2 - \frac{5}{4}\xi_{He'} + \xi_{A'}(\frac{1}{A'} - \frac{3}{2})]} \ . \tag{13}$$

If we vary $\xi_{A'}$ between 0 and 1, then we obtain a lower and upper limit for $v_0^2[A']$:

$$\frac{1}{A'(2 - \frac{5}{4}\xi_{He'})} < \frac{v_0^2[A']}{v_{rot}^2} < \frac{1}{1 + \frac{A'}{2}} \ . \tag{14}$$

Mirror BBN studies[24] indicate that the primordial Helium mass fraction, $Y_{He'}$, is relatively high, with $Y_{He'} \simeq 0.9$, which is quite unlike the case of ordinary matter. However, like the ordinary matter sector, the primordial value for $\xi_{A'}$ is expected[24] to be small $\xi_{A'} \ll 1$. That is, heavy mirror elements are anticipated to be synthesised in mirror stars. If the net A' production from mirror stars remains subdominant, i.e. $\xi_{A'} \ll 1$, then we expect that $v_0[A']$ to be given by the lower limit in Eq.(14) with $\xi_{He'} = Y_{He'} \simeq 0.9$. The situation where $\xi_{A'} \approx 1$ corresponds to extremely efficient mirror star formation and evolution, and is a priori possible. We will therefore consider both limiting cases for $v_0[A']$. It turns out, though, that our results are relatively insensitive to the possible variation of $v_0[A']$ given by Eq.(14) simply because $v_0[A']/v_{rot} << 1$.

4 The DAMA experiment

The DAMA experiments[1, 2, 3] employ large mass scintillation sodium iodide detectors operating in the Gran Sasso National Laboratory. These experiments were initially operating with a target mass of around 100 kg and since 2003 with a target of ~ 250 kg. These experiments have been running for more than 13 years and now have a cumulative exposure of 1.17 ton $\times$ year. Importantly, the DAMA experiments have consistently observed a positive dark matter signal, with statistical significance of around 8.9 σ C.L.[3].

The DAMA experiments utilize the annual modulation signature, which provides a "smoking gun" signal for dark matter. The idea[30] is very simple. The interaction rate must vary periodically since it depends on the Earth's velocity, v_E, which modulates due to the Earth's motion around the Sun. That is,

$$R(v_E) = R(v_\odot) + \left(\frac{\partial R}{\partial v_E}\right)_{v_\odot} \Delta v_E \cos\omega(t - t_0) \tag{15}$$

where $v_\odot = v_{rot} + 12$ km/s is the sun's velocity with respect to the galactic halo and $\Delta v_E \simeq 15$ km/s, $\omega \equiv 2\pi/T$ ($T = 1$ year) with $t_0 = 152.5$ days (from astronomical data). Importantly the phase and period of the modulation are both predicted![6] This gives a strong systematic check on their results. Such an annual modulation has been found in the 2-6 keVee recoil energy region at the 8.9σ confidence level, with T, t_0 measured to be[3]:

$$\begin{aligned} T &= 0.999 \pm 0.002 \text{ year} \\ t_0 &= 146 \pm 7 \text{ day}. \end{aligned} \tag{16}$$

Clearly, both the period and phase are consistent with the theoretical expectations of halo dark matter. There are no known systematic effects which could produce the modulation of the signal seen and thus it is reasonable to believe that the DAMA experiments have detected dark matter.

Mirror dark matter explains the DAMA annual modulation signal via kinetic mixing induced elastic (Rutherford) scattering of the dominant mirror metal component, A', off target nuclei. [The H' and He' components are too light to give a signal above the DAMA energy threshold]. We leave it up to the experimental data to determine $m_{A'}$, although our best 'theoretical' guess would be $A' \sim O'$ given that O is the dominant metal in the ordinary matter sector. The differential interaction rate is given by:

$$\begin{aligned} \frac{dR}{dE_R} &= N_T n_{A'} \int \frac{d\sigma}{dE_R} \frac{f_{A'}(\mathbf{v}, \mathbf{v}_E)}{k} |\mathbf{v}| d^3v \\ &= N_T n_{A'} \frac{\lambda}{E_R^2} \int_{|\mathbf{v}| > v_{min}(E_R)}^{\infty} \frac{f_{A'}(\mathbf{v}, \mathbf{v}_E)}{k|\mathbf{v}|} d^3v \end{aligned} \tag{17}$$

where N_T is the number of target atoms per kg of detector (we must sum over Na and I interactions separately), $k = (\pi v_0^2 [A'])^{3/2}$ is the Maxwellian distribution normalization factor and $n_{A'} = \rho_{dm} \xi_{A'}/m_{A'}$ is the number density of the mirror nuclei A' at the Earth's location (we take $\rho_{dm} = 0.3\ GeV/cm^3$). Here $\mathbf{v}$ is the velocity of the halo particles relative to the Earth and $\mathbf{v}_E$ is the velocity of the Earth relative to the galactic halo. Note that the lower velocity limit, $v_{min}(E_R)$, is

[6]Deviations from $t_0 = 152.5$ days are possible if there is bulk halo rotation. However, a large deviation from the expected value of $t_0 = 152.5$ days would be difficult to reconcile with the inferred approximate spherical distribution of the dark matter in the galactic halo.

given by the kinematic relation:

$$v_{min} = \sqrt{\frac{(m_A + m_{A'})^2 E_R}{2 m_A m_{A'}^2}} \ . \tag{18}$$

The velocity integral in Eq.(17),

$$I \equiv \int_{|\mathbf{v}|>v_{min}(E_R)}^{\infty} \frac{f_{A'}(v)}{k|\mathbf{v}|} d^3v \tag{19}$$

can easily be evaluated in terms of error functions assuming a Maxwellian distribution: $f_{A'}(\mathbf{v}, \mathbf{v}_E)/k = (\pi v_0^2[A'])^{-3/2} exp(-(\mathbf{v}+\mathbf{v}_E)^2/v_0^2[A'])$. In fact,

$$I = \frac{1}{2 y v_0[A']} [erf(x+y) - erf(x-y)] \ , \tag{20}$$

where

$$x \equiv \frac{v_{min}(E_R)}{v_0[A']}, \ y \equiv \frac{v_E}{v_0[A']} \ . \tag{21}$$

The differential interaction rate, Eq.(17), can then be expanded in a Taylor series yielding a time independent part (which we subsequently denote as the 'absolute' rate) and time dependent modulated component:

$$\frac{dR}{dE_R} \simeq \frac{dR^0}{dE_R} + \frac{dR^1}{dE_R} \cos\omega(t - t_0) \ , \tag{22}$$

with

$$\begin{aligned} \frac{dR^0}{dE_R} &= \frac{N_T n_{A'} \lambda I(E_R, y_0)}{E_R^2} \\ \frac{dR^1}{dE_R} &= \frac{N_T n_{A'} \lambda \Delta y}{E_R^2} \left(\frac{\partial I}{\partial y}\right)_{y=y_0} \ . \end{aligned} \tag{23}$$

Here $y_0 = v_\odot / v_0[A'], \ \Delta y = \Delta v_E / v_0[A']$ and

$$\left(\frac{\partial I}{\partial y}\right)_{y=y_0} = -\frac{I(E_R, y_0)}{y_0} + \frac{1}{\sqrt{\pi} y_0 v_0[A']} \left[e^{-(x-y_0)^2} + e^{-(x+y_0)^2}\right] \ . \tag{24}$$

To compare with the measured rates we must take into account the quenching factor and detector resolution. We include detector resolution effects by convolving the rates with a Gaussian:

$$\frac{dR^{0,1}}{dE_R^m} = \frac{1}{\sqrt{2\pi}\sigma_{res}} \int \frac{dR^{0,1}}{dE_R} e^{-(E_R - E_R^m)^2/2\sigma_{res}^2} dE_R \ , \tag{25}$$

where E_R^m is the measured energy. The resolution is given by[31]

$$\frac{\sigma_{res}}{E_R} = \frac{\alpha}{\sqrt{E_R(keVee)}} \; + \; \beta \tag{26}$$

where $\alpha = 0.448 \pm 0.035$, $\beta = (9.1 \pm 5.1) \times 10^{-3}$. The unit of energy is the electron equivalent energy, keVee. For nuclear recoils, in the absence of any channeling, keVee = keV/q_A, where q_A is the quenching factor. For DAMA, $q_{Na} \approx 0.3$ while $q_I \approx 0.09$. Channeled events where target atoms travel down crystal axis and planes have $q_A \simeq 1$.

The issue of channeling has recently been re-examined in ref.[32]. It was found that the channeling fraction is likely to be very small ($< 1\%$) in the energy range of interest in contrast with the earlier study[33] performed by the DAMA collaboration. It is argued that the DAMA analysis did not take into account that the scattered atoms originate from lattice sites and hence cannot be easily channeled. In light of these developments, we expect that the channeling fraction is indeed small - probably negligible. Throughout this paper, therefore, we shall generally assume that no channeling occurs, with the exception of figures 2 and 4 where we compute the allowed region of parameter space and include the channeling region as a comparison.

The measured annual modulation amplitudes for the 1.17 ton-year cumulative exposure, $S_i^m \pm \sigma_i$, are binned into $\Delta E = 0.5$ keVee energy bins and can be obtained from figure 6 of ref.[3]. This is to be compared with the computed annual modulation amplitude for mirror dark matter obtained by averaging the differential rate over the binned energy taking into account the resolution and quenching factors: [7]

$$\frac{\overline{dR}_i^1}{dE_R^m} = \frac{1}{\Delta E} \int_{E_i}^{E_i + \Delta E} \frac{dR^1}{dE_R^m} dE_R^m \; . \tag{27}$$

It is convenient to define a χ^2 quantity:

$$\chi^2(\epsilon\sqrt{\xi_{A'}}, m_{A'}) = \sum \left(\frac{\overline{dR}_i^1}{dE_R^m} - S_i^m \right)^2 / \sigma_i^2 \; . \tag{28}$$

We consider the energy range 2-8 keVee, separated into 12 bins of width 0.5 keVee, which encompasses the 2-6 keVee DAMA signal region. Varying the parameters $m_{A'}, \epsilon\sqrt{\xi_{A'}}$ around the best fit, we can obtain the DAMA allowed region[8]. There are a number of systematic uncertainties which can be included in the analysis and we have examined the following: a) considering $v_0[A']$ within its expected limits given by Eq.(14), b) varying the quenching factors for Iodine and sodium by $\pm 20\%$, i.e. taking $q_{Na} = 0.30 \pm 0.06$ and $q_I = 0.09 \pm 0.02$, c) varying the detector resolution over

[7] The DAMA data are efficiency corrected so there is no need to include the detection efficiency in Eq.(27).

[8] For the purposes of the fit, we analytically continue the mass number, A', to non-integer values, with $Z' = A'/2$. Since the realistic case will involve a spectrum of elements, the effective mass can be non-integer

its 2σ uncertainty and d) varying $v_{rot} = 254 \pm 32$ km/s, that is around $\pm 2\sigma$ from its estimated value. The variation of quenching factor and resolution were taken into account by minimizing $\chi^2(q_I, q_{Na}, \sigma_{res}, m_{A'}, \epsilon\sqrt{\xi_{A'}})$ over 20% variation of q_I and q_{Na}, and over the 2σ uncertainty in σ_{res}. This defines $\bar{\chi}^2(m_{A'}, \epsilon\sqrt{\xi_{A'}})$. The best fit for DAMA has $\bar{\chi}^2_{min} \simeq 8.5$ for 10 degrees of freedom. Some examples near the best fit, assuming no channeling occurs, are shown in figure 1.

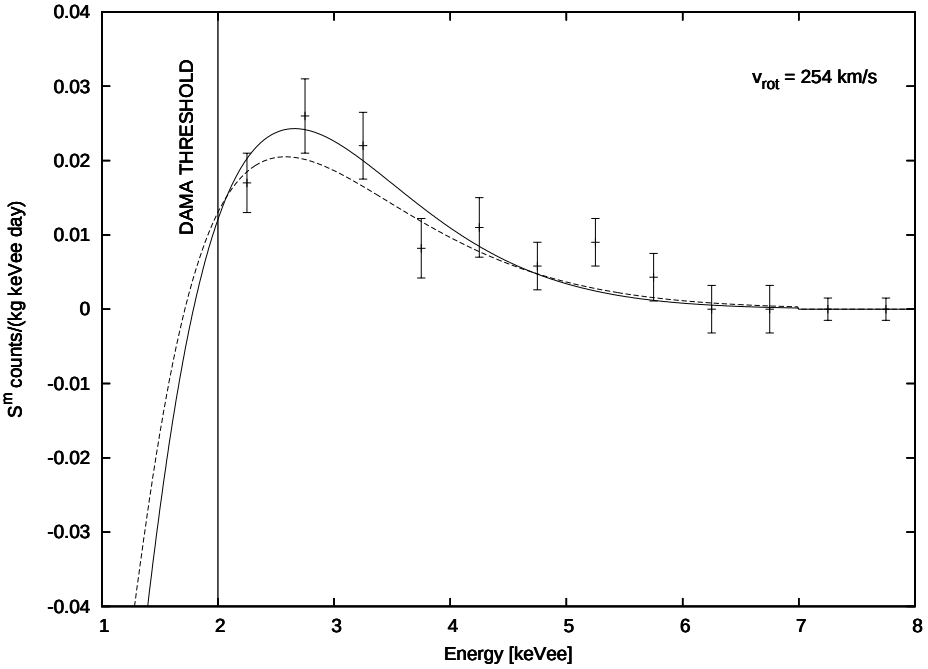

Figure 1: DAMA annual modulation amplitude versus measured recoil Energy for the parameters: $m_{A'}/m_p = 20$, $\epsilon\sqrt{\xi_{A'}} = 7.4 \times 10^{-10}$ and $v_{rot} = 254$ km/s. The solid (dashed) line corresponds to the lower (upper) $v_0[A']$ limit given in Eq.(14). Negligible channeling has been assumed.

Favoured regions in the $m_{A'}, \epsilon\sqrt{\xi_{A'}}$ plane can be obtained by evaluating the contours with $\bar{\chi}^2 = \bar{\chi}^2_{min} + 9$ (roughly 99% C.L.). In figure 2 we plot the allowed regions for DAMA assuming $v_{rot} = 222$ km/s [fig 2a], $v_{rot} = 254$ km/s [fig 2b] and $v_{rot} = 286$ km/s [fig 2c] . Also shown in the figures are the DAMA allowed region assuming that channeling occurs with fractions as originally estimated by the DAMA collaboration[33]. It has been emphasised recently[34] that the systematic uncertainty in q_{Na} might be as large as $q_{Na} = 0.30 \pm 0.13$ given the lack of measurements of the quenching factor in the low energy region. If this is the case, then we find that the favoured regions extend out to somewhat ($\approx 10 - 15\%$) lower $m_{A'}$ values than that given in figure 2.

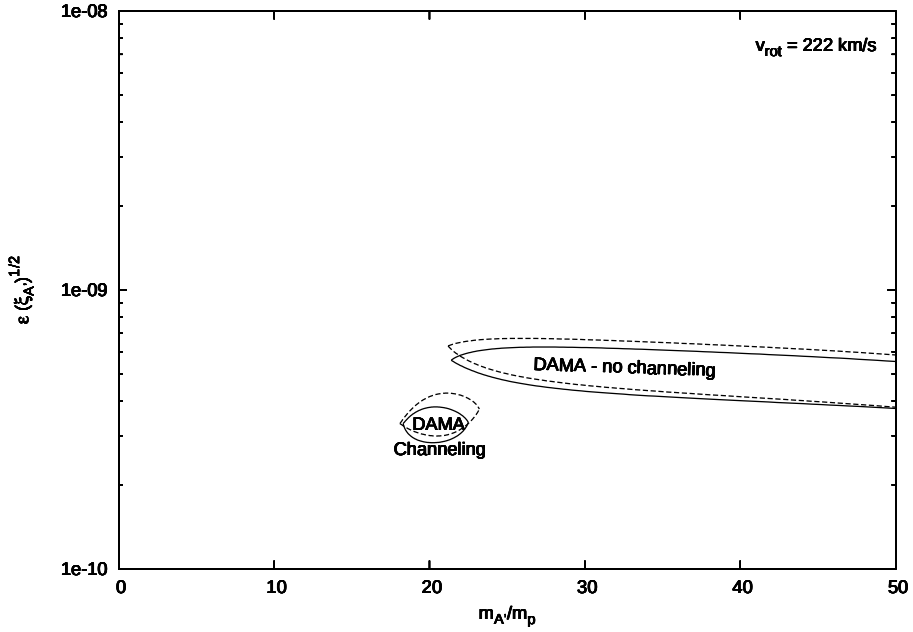

Figure 2a: DAMA [99% C.L.] allowed region in the $m_{A'}, \epsilon\sqrt{\xi_{A'}}$ plane, assuming negligible channeling fraction, for $v_{rot} = 222$ km/s. Solid (dashed) line corresponds to the lower (upper) $v_0[A']$ limit given in Eq.(14). Also shown for comparison is the DAMA allowed regions if channeling occurs with fractions originally estimated by the DAMA collaboration.

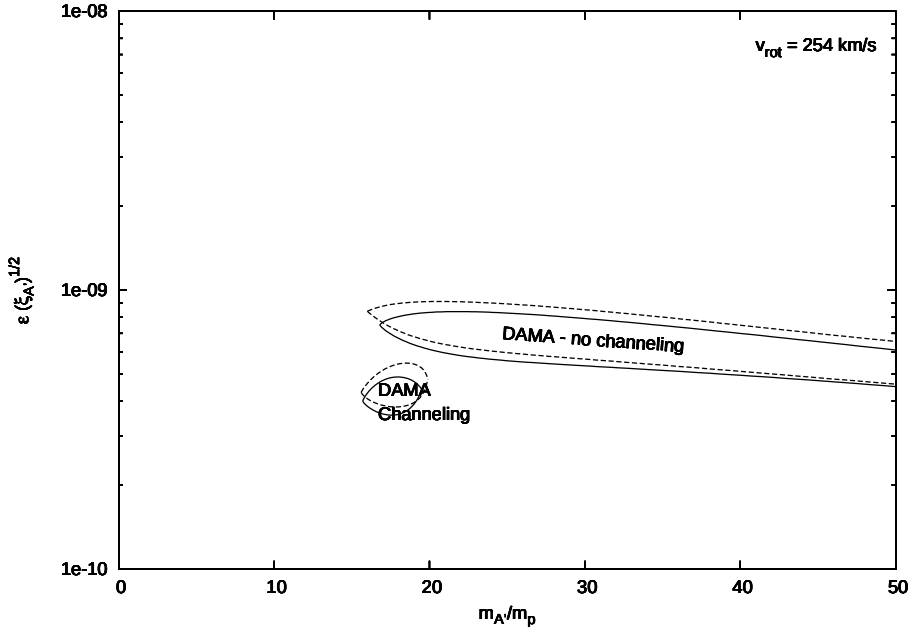

Figure 2b: Same as figure 2a, except with $v_{rot} = 254$ km/s.

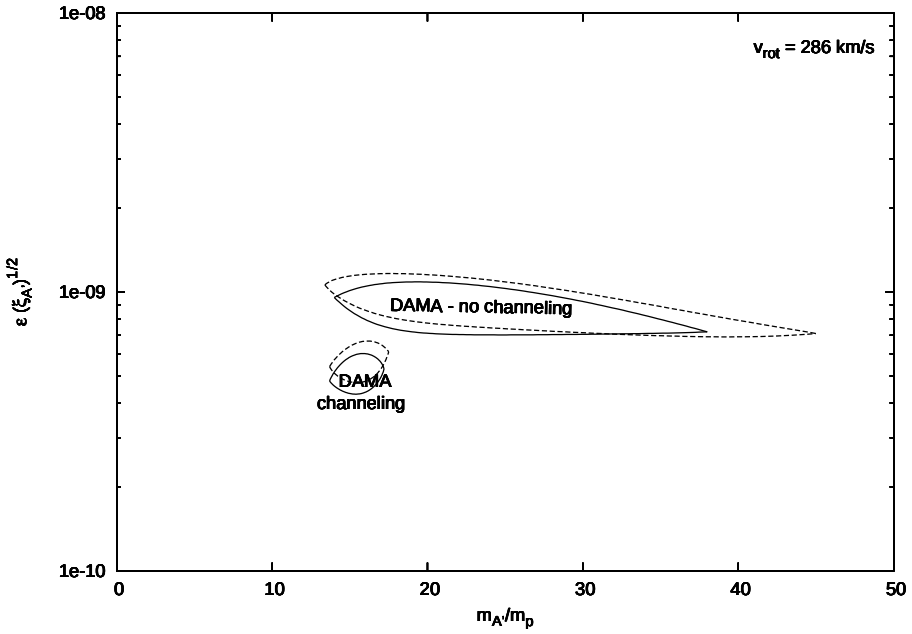

Figure 2c: Same as figure 2a, except with $v_{rot} = 286$ km/s.

The main features of the annual modulation spectrum predicted by A' dark matter can be easily understood. As discussed earlier[10], at low E_R, where $x(E_R) \ll y$, dR^1/dE_R is negative. As E_R increases, dR^1/dE_R changes sign and reaches a maximum at the value of E_R where $x(E_R) \approx y$, or equivalently, the value of E_R where $v_{min}(E_R) = v_{rot}$. At high E_R ($x \gg y$), $dR^1/dE_R \to 0$. From Eq.(18) this means that the position of the peak, E_R^{peak}, is given by:

$$E_R^{peak} \approx \frac{2m_A m_{A'}^2}{(m_A + m_{A'})^2} v_{rot}^2 \ . \tag{29}$$

For low $m_{A'} \lesssim 30m_p$ the annual modulation signal arises predominantly from A' scattering with Na, while for $m_{A'} \gtrsim 30m_p$ scattering off both Na and I contributes significantly to produce the signal[9]. Note that since $v_0[A'] \ll v_{rot}$ the velocity distribution is so narrow that the width of the peak is dominated by the detector resolution. This explains the relative insensitivity of the fit to the particular $v_0[A']$ value which is evident in figures 1,2.

To summarize, we see that without channeling the DAMA annual modulation signal can be explained for a relatively wide range of $m_{A'}$ values, which includes the region around $m_{A'}/m_p \sim 16$, expected if $A' = O'$ dominates the mirror metal

[9]In the case where channeling is assumed with the fractions originally estimated by the DAMA collaboration[33] the annual modulation signal is dominated by interactions with I only. See ref.[10] for further discussion of this case.

component. We now turn to the positive low energy excess observed by CoGeNT, together with the implications from the null experiments, such as XENON100 and CDMS/Si.

5 The CoGeNT experiment

The CoGeNT experiment operating in the Soudan Underground Laboratory has recently presented new results in their search for light dark matter interactions[4]. With a low energy threshold of 0.4 keVee and a Germanium target, they have observed a low energy excess which is not easily explainable in terms of known background sources. The energy region probed by CoGeNT overlaps with the energy region in which the DAMA collaboration have observed their impressive annual modulation signal and thus it is natural to interpret the CoGeNT low energy excess in terms of A' mirror dark matter interactions. In ref.[13] we showed that the CoGeNT excess is compatible with mirror dark matter expectations and thus provides a model dependent check of the DAMA signal, which we now examine in more detail.

To compare with the measured event rate, we include detector resolution effects and overall detection efficiency:

$$\frac{dR^0}{dE_R^m} = \epsilon_f(E_R^m)\frac{1}{\sqrt{2\pi}\sigma}\int \frac{dR^0}{dE_R} e^{-(E_R-E_R^m)^2/2\sigma^2} dE_R \tag{30}$$

where E_R^m is the measured energy and $\sigma^2 = \sigma_n^2 + (2.35)^2 E_R \eta F$ with $\sigma_n = 69.4$ eV, $\eta = 2.96$ eV and $F = 0.29$[4, 35]. The detection efficiency, $\epsilon_f(E_R^m)$, was given in figure 3 of ref.[4], which we approximate via

$$\epsilon_f(E_R^m) \simeq \frac{0.87}{1 + (0.4/E_R^m)^6}. \tag{31}$$

The energy is in keVee units (ionization energy). For nuclear recoils in the absence of any channeling, $keVee = keV/q$, where $q \simeq 0.21$ is the relevant quenching factor in the near threshold region[34].

We fit the CoGeNT data in the low recoil energy range assuming A' dark matter and that the background is an energy independent constant, together with two Gaussians to account for the ^{65}Zn (1.1 keV) and ^{68}Ge (1.29 keV) L-shell electron capture lines. Initially fixing $m_{A'}/m_p = 20$ and $v_{rot} = 254$ km/s, as an example, we find a best fit of $\chi^2_{min} \simeq 14.8$ for $21 - 4 = 17$ degrees of freedom, with $\epsilon\sqrt{\xi_{A'}} = 6.2 \times 10^{-10}$ (independently of whether we take the upper or lower limiting values of v_0). This fit for CoGeNT is shown in figure 3.

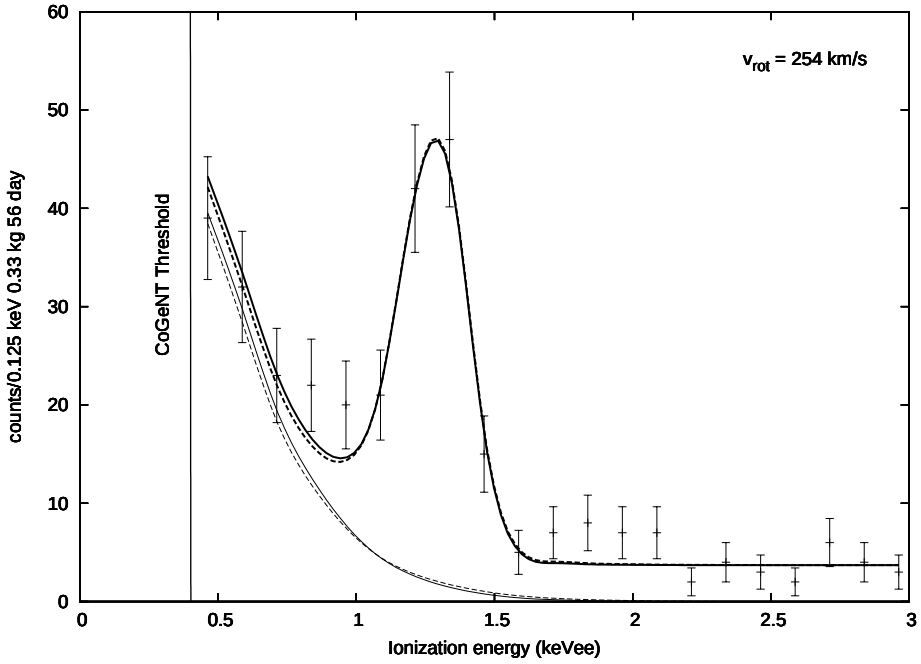

Figure 3: Fit of the CoGeNT spectrum for $m_{A'}/m_p = 20$, $\epsilon\sqrt{\xi_{A'}} = 6.2 \times 10^{-10}$ and $v_{rot} = 254$ km/s. Thick solid (dashed) line is with lower (upper) $v_0[A']$ limit given in Eq.(14). Also shown is the dark matter contribution to the signals (thin lines). Negligible channeling has been assumed.

The shape of the spectrum is nicely fit by A' dark matter due primarily to the E_R dependent Rutherford cross section: $d\sigma/dE_R \propto 1/E_R^2$. As further data is collected this E_R dependence will be more stringently constrained, which will pose a more rigorous test of the mirror dark matter theory.

As in the DAMA case, to account for some of the possible systematic uncertainties we vary the quenching factor by $\pm 20\%$ [i.e. take $q_{Ge} = 0.21 \pm 0.04$]. We define a χ^2 function,

$$\chi^2(q_{Ge}, \epsilon\sqrt{\xi_{A'}}, m_{A'}) = \sum \left(\frac{\overline{dR_i}^0}{dE_R^m} - data_i \right)^2 / \sigma_i^2 \qquad (32)$$

where $\frac{\overline{dR_i}^0}{dE_R^m}$ is the differential rate averaged over the binned energy. We take the experimental errors to be purely statistical, so that $\sigma_i = \sqrt{data_i}$. We minimize $\chi^2(q_{Ge}, m_{A'}, \epsilon\sqrt{\xi_{A'}})$ over the 20% variation in q_{Ge}, which defines $\overline{\chi}^2(m_{A'}, \epsilon\sqrt{\xi_{A'}})$. Of course, we also minimize χ^2 with respect to the parameters of the background model describing the amplitudes of the ^{65}Zn (1.1 keV) and ^{68}Ge (1.29 keV) L-shell electron capture lines and adjusting also the constant background component. Note that no

background exponential is assumed (or needed) to fit the data. The CoGeNT allowed region in the $m_{A'}, \epsilon\sqrt{\xi_{A'}}$ plane is then defined via contours $\bar{\chi}^2 = \bar{\chi}^2_{min} + 9$ (roughly 99% C.L.).

In figure 4 we plot the allowed regions for CoGeNT together with the DAMA allowed region for $v_{rot} = 222$ km/s [fig 4a], $v_{rot} = 254$ km/s [fig 4b] and $v_{rot} = 286$ km/s [fig 4c] . We have allowed for a 20% systematic uncertainty in both CoGeNT and DAMA quenching factors. In these figures we have assumed $\xi_{A'} \ll 1$ so that $v_0[A']$ is given by the lower limit given in Eq.(14). The case where $\xi_{A'} \simeq 1$ features an almost indistinguishable allowed region (as already illustrated in figure 2 for the case of DAMA), so is not given. Also shown are the corresponding 95% C.L. exclusion limits from CDMS/Si[36], CDMS/Ge[5] and XENON100[37] experiments.

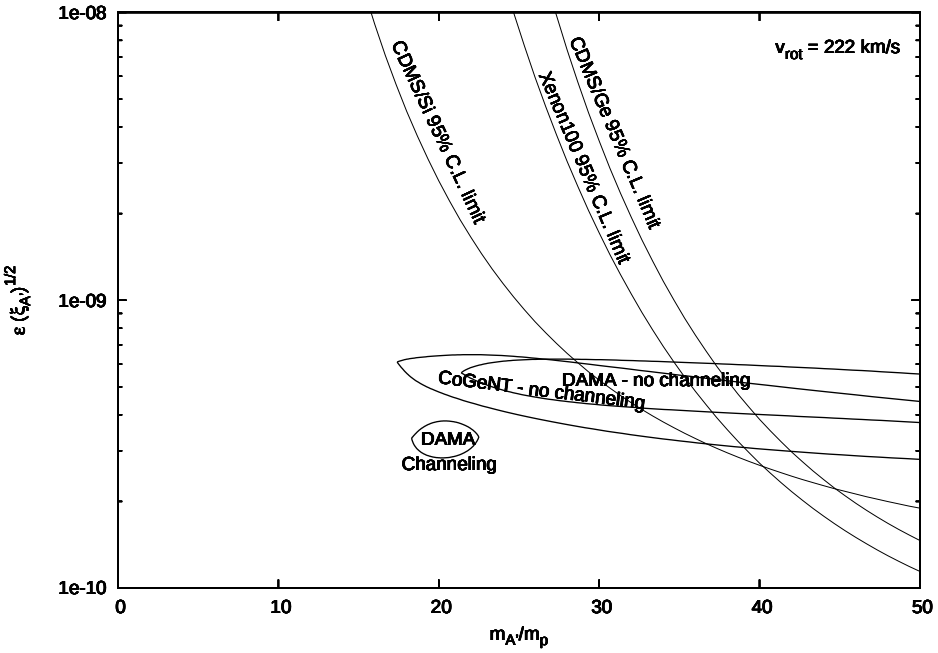

Figure 4a: DAMA and CoGeNT [99% C.L.] allowed regions in the $m_{A'}/m_p$, $\epsilon\sqrt{\xi_{A'}}$ plane, assuming negligible channeling fraction, for $v_{rot} = 222$ km/s. Also shown are a) DAMA allowed regions if channeling occurs with fractions originally estimated by the DAMA collaboration and b) the exclusion limits from CDMS/Si, CDMS/Ge and XENON100 experiments. [The region excluded is to the right of the exclusion limits].

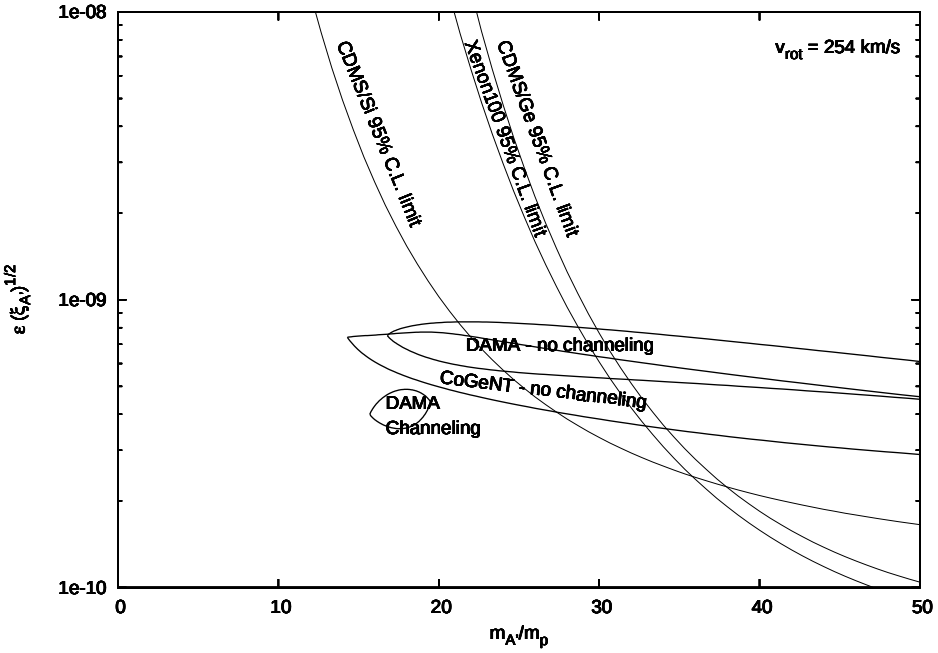

Figure 4b: Same as figure 4a, except with $v_{rot} = 254$ km/s.

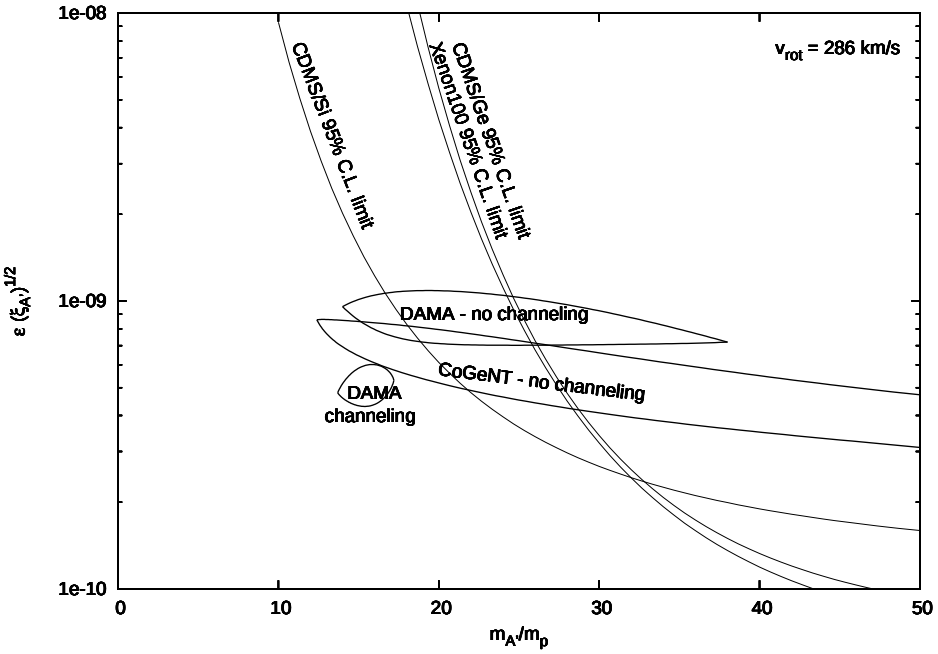

Figure 4c: Same as figure 4a, except with $v_{rot} = 286$ km/s.

In computing the exclusion limits we have allowed for a 20% systematic uncertainty in energy threshold. That is, the threshold for CDMS/Si[36] was taken to be 8.4 keV_{nr} rather than the quoted 7.0 keV_{nr}, the threshold for CDMS/Ge[5] was taken to be 12 keV_{nr} rather than the quoted 10 keV_{nr} and the threshold for XENON100[37] was taken to be 10.4 keV_{nr} rather than the quoted 8.7 keV_{nr}[10]. For the CDMS/Si experiment, we used the quoted[36] raw exposure of 33.9 kg-days for $E_R < 10\ keV_{nr}$, 38.8 kg-days for $10 < E_R(keV_{nr}) < 15$ and 53.5 kg-days for $E_R > 15\ keV_{nr}$, and assumed a detection efficiency of 20% in the energy region near threshold. For the CDMS/Ge experiment we assumed the total raw exposure of 1010 kg-days and a detection efficiency of $\epsilon_f = 0.18 + 0.007E_R$ in the low energy region of interest[5]. For the XENON100 experiment we used the quoted[37] raw exposure of 447 kg-days together with a detection efficiency of 0.4 in the low energy region.

From figure 4 it is evident that the CDMS/Si experiment is the most sensitive of the null experiments to A' dark matter, which is due to its light target element and relatively low threshold. The CDMS/Si experiment constrains the allowed region to $m_{A'}/m_p \lesssim 30$. Observe also that the CDMS/Si experiment seems to exclude the two events seen in the CDMS/Ge experiment[5] as being due to the same component which can explain the DAMA and CoGeNT data. It is possible, though, to interpret the two events seen by CDMS/Ge as a hint of a heavier $\sim Fe'$ component. This interpretation requires[12] $\xi_{Fe'}/\xi_{A'} \sim 10^{-2}$ and is not excluded by CDMS/Si or any other experiment. Such a small Fe' component does not significantly affect the fit of the DAMA or CoGeNT experiments. We will examine the effects of the Fe' component for the higher threshold experiments in more detail in section 7.

We have also performed a global analysis of the DAMA and CoGeNT signals. Fixing $v_{rot} = 254$ km/s and evaluating χ^2 for the combined DAMA+CoGeNT data, we have found $\chi^2_{min} = 24.4$ for 28 d.o.f. at $m_{A'}/m_p = 24$, $\epsilon\sqrt{\xi_{A'}} = 6.4 \times 10^{-10}$. Excellent fits to the combined DAMA and CoGeNT data are also obtained for $v_{rot} = 222$ km/s and $v_{rot} = 286$ km/s. In figure 5 we plot the favoured region of parameter space for the combined fit of the DAMA and CoGeNT data for three representative values of v_{rot}.

[10]Exclusion limits from the XENON10 experiment are only marginally better than the XENON100 exclusion limit (but not better than the CDMS/Si limit). For a recent discussion about the calibration and other uncertainties in the XENON low energy region, see ref.[38].

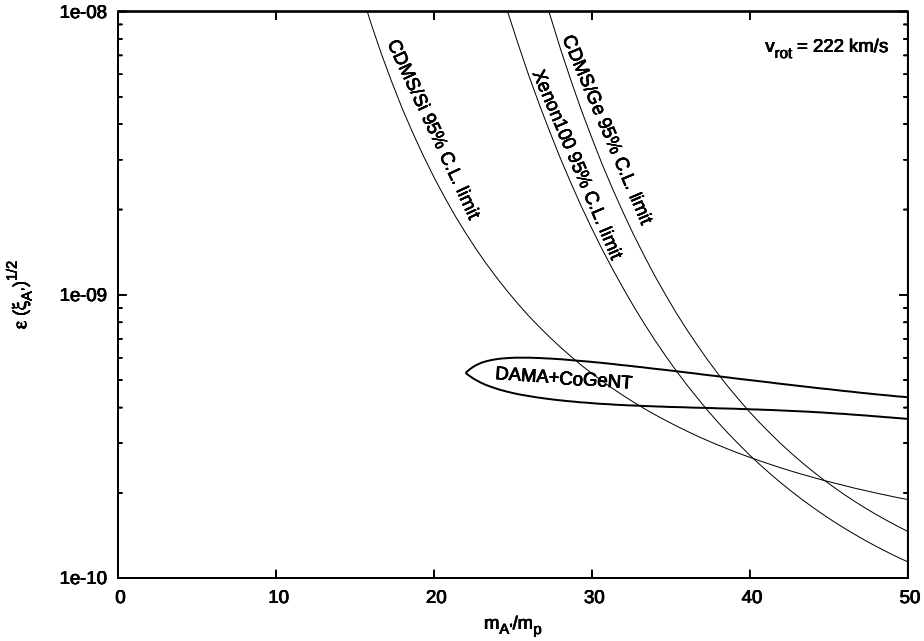

Figure 5a: DAMA and CoGeNT [99% C.L.] global allowed region in the $m_{A'}/m_p$, $\epsilon\sqrt{\xi_{A'}}$ plane, assuming negligible channeling fraction, for $v_{rot} = 222$ km/s. Also shown are the exclusion limits from CDMS/Si, CDMS/Ge and XENON100 experiments. [The region excluded is to the right of the exclusion limits].

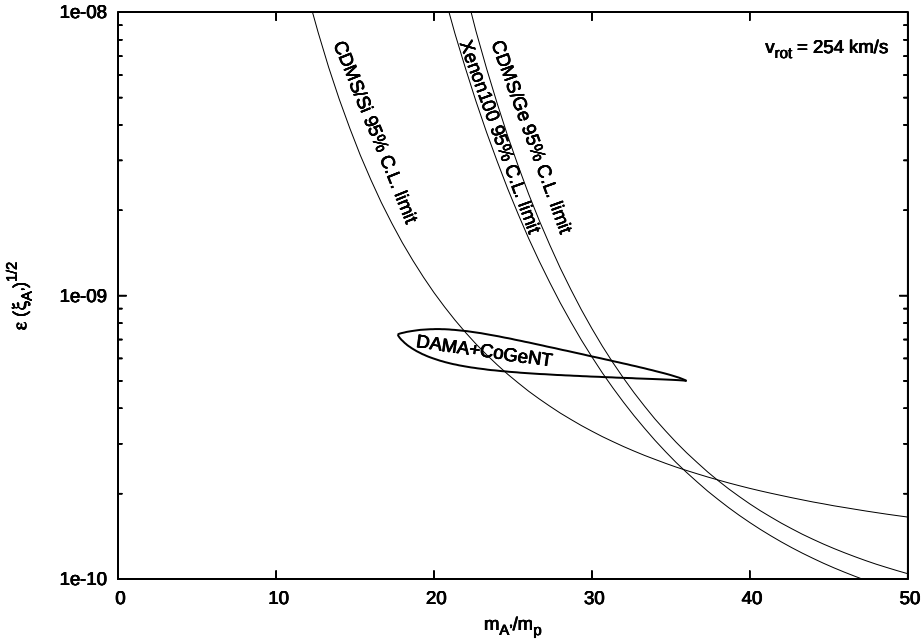

Figure 5b: Same as figure 5a except that $v_{rot} = 254$ km/s.

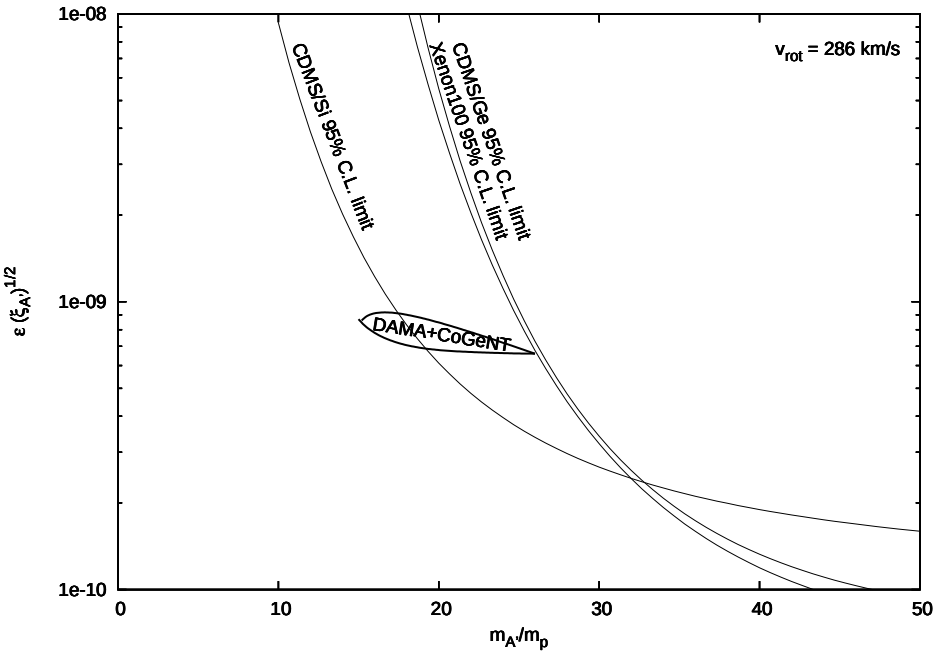

Figure 5c: Same as figure 5a except that $v_{rot} = 286$ km/s.

The CoGeNT experiment has been running continuously since December 2009, and might collect enough data to search for the annual modulation signal. In figure 6 we show results for the annual modulation amplitude predicted for the CoGeNT experiment. Interestingly we see that there is a change of sign for the annual modulation amplitude at low energies $E_R \approx 0.5 - 0.8$ keVee (depending on the parameters). This means that at the lowest energies CoGeNT should see *more* events during the (northern) winter/fall than the (northern) summer/spring. This might provide a useful means of experimentally distinguishing this dark matter theory from other possible explanations.

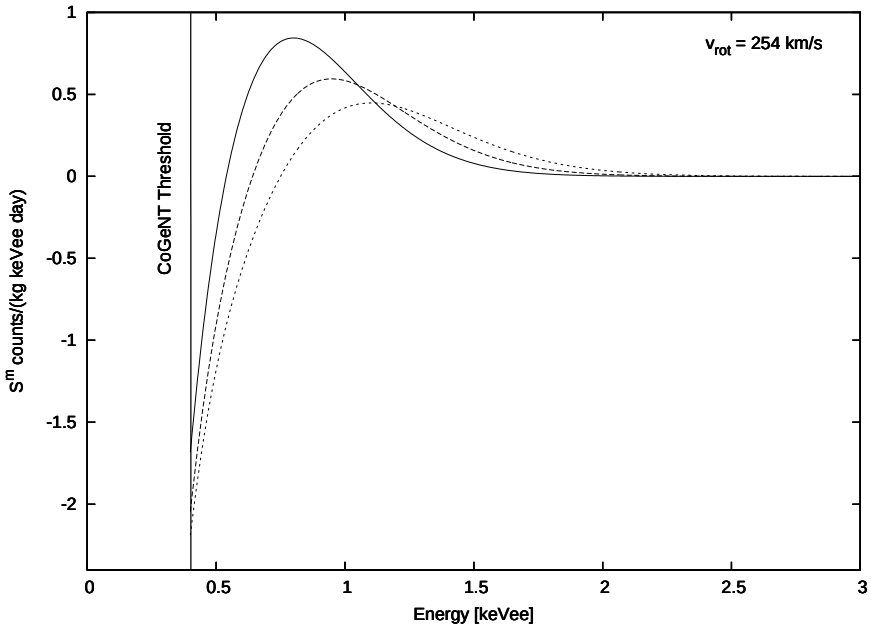

Figure 6: CoGeNT annual modulation amplitude versus recoil energy. For some representative parameters: $\epsilon\sqrt{\xi_{A'}} = 7.0 \times 10^{-10},\ m_{A'}/m_p = 18$ (solid line), $\epsilon\sqrt{\xi_{A'}} = 6.4 \times 10^{-10},\ m_{A'}/m_p = 20$ (dashed line), $\epsilon\sqrt{\xi_{A'}} = 6.0 \times 10^{-10},\ m_{A'}/m_p = 22$ (dotted line). All for $v_{rot} = 254$ km/s. The figure assumes 100% detection efficiency.

6 Electron scattering and the DAMA absolute rate

In addition to nuclear recoils, electron recoils from mirror electron scattering off bound atomic electrons in the target volume can also occur. The e' component of the halo is expected to be distributed with Maxwellian velocity distribution, and since $m_{e'} \ll \bar{m}$, we expect $v_0[e'] \gg v_{rot}$. In fact, from Eqs.(11,12) we can estimate that $v_0[e']$ is in the range:

$$\left[\frac{m_p}{m_e}\right] \frac{1}{2 - \frac{5}{4}\xi_{He'}} \lesssim \frac{v_0^2[e']}{v_{rot}^2} \lesssim \left[\frac{m_p}{m_e}\right] \frac{A'}{1 + A'/2} \ . \tag{33}$$

Since $v_0[e'] \gg v_{rot}$ we can, to a good approximation, neglect v_{rot} when dealing with $e' - e$ scattering. This means that electron recoils give a negligible contribution to the annual modulation signal, however they can contribute significantly to the absolute rate at energies below 2 keVee. Interestingly such a rise at low energies was observed in the CDMS electron scattering data[6] and is compatible with $\epsilon \sim 10^{-9}$[11]. Recall that the DAMA experiment doesn't discriminate against electron recoils, so the DAMA experiment is also sensitive to electron recoils through their contribution to the absolute rate as we now discuss.

The DAMA experiment constrains the absolute event rate to be less than around 1 cpd/kg/keVee in the region near threshold. We shall here examine the implications of this constraint for mirror dark matter. As discussed above, we expect both nuclear recoils and electron recoils to contribute to the absolute rate from dark matter interactions. The nuclear recoil contribution can easily by calculated as in Eq.(25). The electron recoil contribution is more complicated. An accurate treatment of the cross section would require knowledge of the wavefunctions of all the electrons in the Na and I atoms. A rough estimate of the electron scattering contribution can be made by[11] considering only the contribution of the loosely bound (binding energy less than 0.1 keV) outer shell electrons in Na and I. The number of such loosely bound atomic electrons is 9 for Na and 17 for I. We further approximate these electrons as free and at rest, and compute the elastic scattering rate on these electrons. Thus, within this approximation the cross section has the form given in Eq.(6), with $\lambda_e = 2\pi\epsilon^2\alpha^2/m_e$. The predicted differential interaction rate is then:

$$\begin{aligned} \frac{dR}{dE_R} &= gN_T n_{e'} \int \frac{d\sigma}{dE_R} \frac{f_{e'}(v)}{k} |v| d^3v \\ &= gN_T n_{e'} \frac{\lambda_e}{E_R^2} \int_{|v|>v_{min}(E_R)}^{\infty} \frac{f_{e'}(v)}{k|v|} d^3v \end{aligned} \tag{34}$$

where N_T is the number of target NaI pairs per kg of detector and $k = (\pi v_0^2[e'])^{3/2}$ is the Maxwellian distribution normalization factor. The quantity $g = 26$, is the number of loosely bound atomic electrons per NaI pair as we discussed above. Also, $n_{e'}$ is the halo e' number density. Assuming the halo is fully ionized it is straightforward to show that

$$n_{e'} = \left[1 - \frac{\xi_{He'}}{2} - \frac{\xi_{A'}}{2}\right] \frac{\rho_{dm}}{m_p} \, . \tag{35}$$

Note that the lower velocity limit in Eq.(34), $v_{min}(E_R)$, is given by the kinematic relation:

$$v_{min} = \sqrt{\frac{2E_R}{m_e}}. \tag{36}$$

The velocity integral in Eq.(34) can be analytically solved leading to:

$$\frac{dR}{dE_R} = gN_T n_{e'} \frac{\lambda_e}{E_R^2} \left(\frac{2e^{-x^2}}{\sqrt{\pi} v_0[e']} \right) \tag{37}$$

where $x = v_{min}/v_0[e']$. Finally, to compare with the experimentally measured rate we convolve this rate, with a Gaussian [as in Eq.(25)] to take into account the finite detector resolution.

There are many potential systematic uncertainties in the absolute rate, and we consider the following: the uncertainty in the measured detector resolution [i.e.

taking a 2σ variation of the measured σ_{res} given in Eq.(26)], a $\sim 30\%$ uncertainty in the $e' - e$ scattering cross section, and a 0.25 keVee uncertainty in energy calibration.

In figure 7 we give an example of the absolute rate predicted for the DAMA experiment showing both electron and nuclear recoil contributions separately, using the aforementioned systematic uncertainties to minimize the rate. Since the data below 2 keVee is formally below the DAMA threshold we do not attempt to fit this data, and must await the forthcoming DAMA upgrade which is designed to lower the energy threshold. The rise in event rate below 2 keVee, which is illustrated in figure 7, is a prediction of this model which DAMA can potentially confirm when they lower their energy threshold.

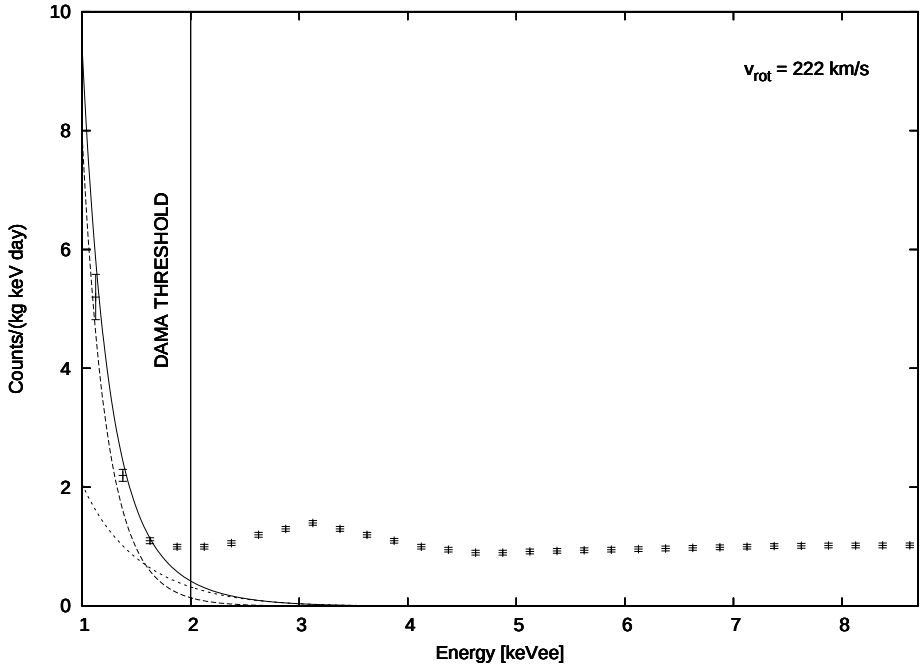

Figure 7: DAMA absolute rate from nuclear recoils with negligible channeling (dotted line), electron recoils (dashed line) and combined (solid line) for the parameters: $m_{A'}/m_p = 20$, $\epsilon\sqrt{\xi_{A'}} = 5.0 \times 10^{-10}$ and $\epsilon = 1.0 \times 10^{-9}$ ($\Rightarrow \xi_{A'} = 0.25$). $v_{rot} = 222$ km/s has been assumed.

In figure 8, we given an example of the electron scattering rate predicted for the CDMS Germanium electron scattering experiment[6], for the same parameters as chosen for figure 7, together with a simple linear model for the background ($R(background) = 1.9 - 0.09E_R$). For the Germanium experiment the resolution is given by[6]

$$\sigma = \sqrt{(0.293)^2 + (0.056)^2 E_R/keV}\ keV \tag{38}$$

and the rate as in Eq.(37) but with $g = 14$[11]. [11].

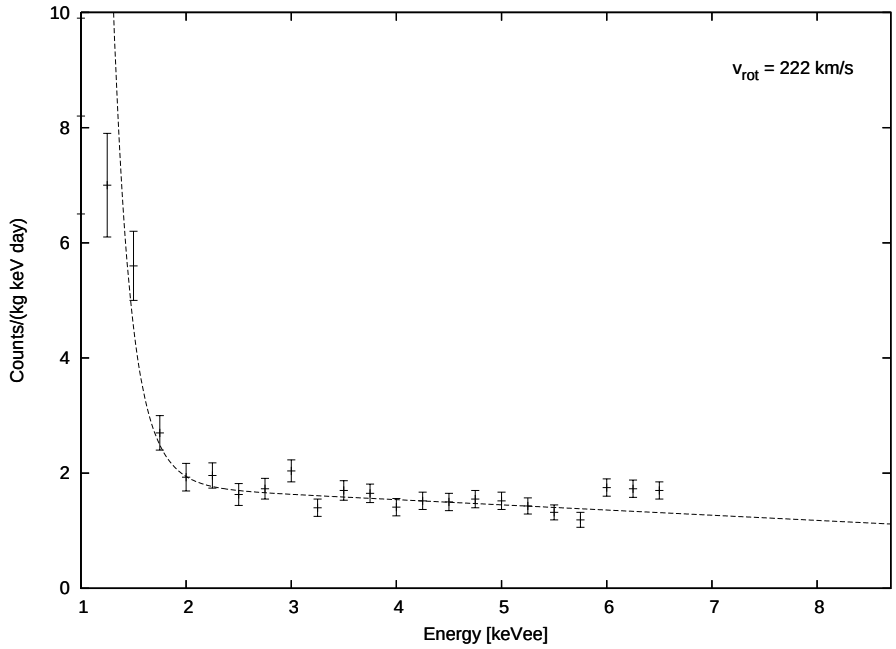

Figure 8: CDMS/Ge absolute rate from electron recoils for the same parameters as figure 7, together with a simple linear background model.

The rise in event rate seen below 2 keV in both DAMA and CDMS electron scattering data is very interesting, but is formally below the threshold of both of these experiments, and therefore needs to be confirmed by future measurements. Conservatively, the only limit that we can obtain is by looking at the data above 2 keV. Demanding that the total rate in the first energy bin above threshold be less than 1 cpd/kg/keV, suggests an upper limit for ϵ. This upper limit depends quite sensitively on the value of $v_0[e']$ (and hence also on v_{rot} and $\xi_{A'}$). If $\xi_{A'} \ll 1$, then

[11] In ref.[11], we assumed a cutoff at $E_R = 0.8$ keV. However this is, in fact unjustified, and here we have no such cutoff except for a phenomenological cutoff at $E_R = 0.2$ keV. Such a low energy cutoff is necessary due to the divergence of the cross section in the $E_R \to 0$ limit.

we find:

$$\begin{aligned}
\epsilon &\lesssim 2.7 \times 10^{-9} \quad , \quad \text{if } \mathrm{v_{rot}} = 222 \text{ km/s} \\
\epsilon &\lesssim 1.5 \times 10^{-9} \quad , \quad \text{if } \mathrm{v_{rot}} = 254 \text{ km/s} \\
\epsilon &\lesssim 1.0 \times 10^{-9} \quad , \quad \text{if } \mathrm{v_{rot}} = 286 \text{ km/s}
\end{aligned} \tag{39}$$

If $\xi_{A'} \approx 1$ then we find:

$$\begin{aligned}
\epsilon &\lesssim 1.1 \times 10^{-9} \quad , \quad \text{if } \mathrm{v_{rot}} = 222 \text{ km/s} \\
\epsilon &\lesssim 0.8 \times 10^{-9} \quad , \quad \text{if } \mathrm{v_{rot}} = 254 \text{ km/s} \\
\epsilon &\lesssim 0.6 \times 10^{-9} \quad , \quad \text{if } \mathrm{v_{rot}} = 286 \text{ km/s.}
\end{aligned} \tag{40}$$

In computing these upper limits we have allowed for some of the systematic uncertainties by including: the uncertainty in the measured detector resolution [i.e. taking a 2σ variation of the measured σ_{res} given in Eq.(26)], a $\sim 30\%$ uncertainty in the $e' - e$ scattering cross section, and a 0.25 keV uncertainty in energy calibration. It should be emphasized, though, that the systematic uncertainty can potentially be much larger in view of the large event rate at low energies which is smeared into $E_R \gtrsim 2$ keV by the resolution. In particular the resolution has not been measured at $E_R \lesssim 2$ keVee and the naive extrapolation might breakdown at low energies. It is also possible that the resolution might fall off faster than a Gaussian in the tails of the distribution, which would weaken the above limits on ϵ. Finally, astrophysical uncertainties in modelling the halo will add further systematic uncertainties to the $e' - e$ scattering rate due to its sensitive dependence on $v_0[e']$. Departures from spherical symmetry or a rotating halo etc will lead to deviations from Eq.(10), and hence to $v_0[e']$. [Note though that the A' scattering rate is much less sensitive to uncertainties in v_0 since $v_0[A'] \ll v_{rot}$, and thus such uncertainties will have little affect on our DAMA/CoGeNT fit]. Thus, given these systematic uncertainties our limits on ϵ should be viewed more as a guide, than strict upper limits.

Similar limits to the above, with the same caveats regarding potentially larger systematic uncertainties, can be obtained from the CDMS electron scattering data. In combination with our estimate of $\epsilon\sqrt{\xi_{A'}} \approx (7 \pm 3) \times 10^{-10}$ from the DAMA and CoGeNT experiments, the limits given in Eq.(40) indicate $\xi_{A'} \gtrsim 10^{-2}$ at $v_{rot} = 222$ km/s, with stronger bounds at higher v_{rot} values. This suggests that the mirror sector may have a higher metal content than the ordinary matter sector. This is certainly possible, and might be due to a period of rapid mirror star formation and evolution during the first few billion years of the Universe (which is suspected given the computed high primordial $Y_{He'} \approx 0.9$ abundance[24] which would dramatically speed up mirror star evolution by several orders of magnitude[25]).

7 CDMS/Ge, EdelweissII and CRESSTII

The CDMS/Ge and EdelweissII experiments utilize a Germanium target, and both of these experiments have found evidence for dark matter interactions. Due to their

relatively high threshold of 10 keV_{nr} for CDMS/Ge and 20 keV_{nr} for Edelweiss, these experiments are not sensitive to the the dominant A' component. The light mass and narrow velocity dispersion of the A' component ensure that the predicted rate for these experiments is much less than 1 event for their net exposures of approximately 200 kg-days and 322 kg-days respectively. However, these experiments are sensitive to heavier mirror dark matter components of the halo, and provide the most sensitive probes of the anticipated Fe' component.

In figure 9 we have given an example of the recoil energy spectrum predicted for CDMS/Ge (figure 9a) and for EdelweissII (figure 9b). The numerical work assumed the CDMS/Ge[5] (EdelweissII[8]) resolution was given by $\sigma_{res} = 0.2$ keV ($\sigma_{res} = 1.0$ keV) and detection efficiency, $eff = 0.18 + 0.007 E_R$ ($eff \simeq 1$). The value for $v_0[Fe']$ was obtained from Eq.(13) assuming that $\xi_{A'} \ll 1$, i.e.

$$v_0^2[Fe'] = \frac{v_{rot}^2}{[m_{Fe}/m_p][2 - \frac{5}{4}\xi_{He'}]} \tag{41}$$

where $\xi_{He'} \approx 0.9$.

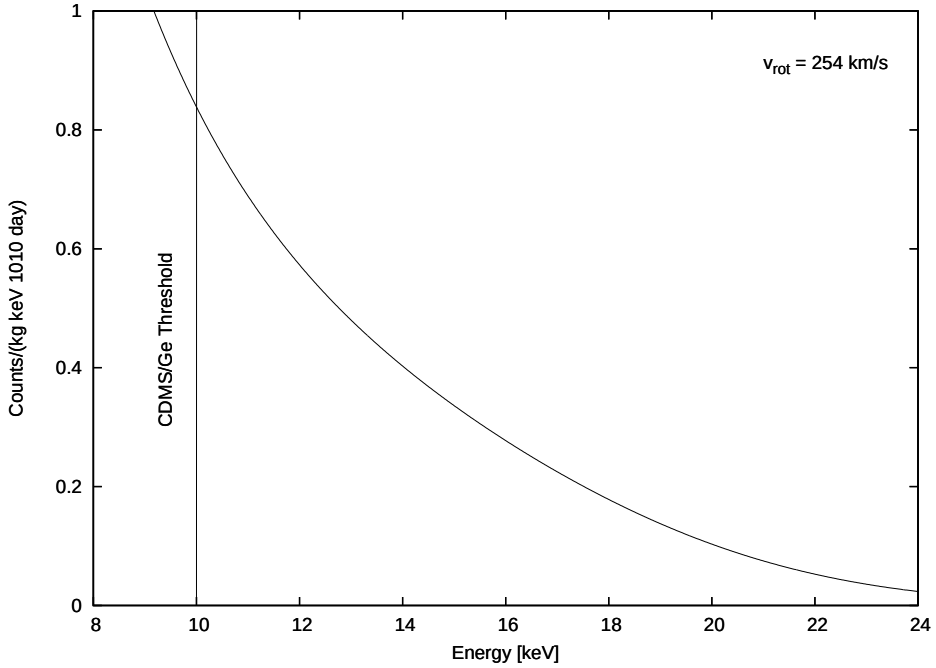

Figure 9a: CDMS/Ge spectrum for Fe' dark matter with $\epsilon\sqrt{\xi_{Fe'}} = 5.0 \times 10^{-11}$. We have assumed $v_{rot} = 254$ km/s.

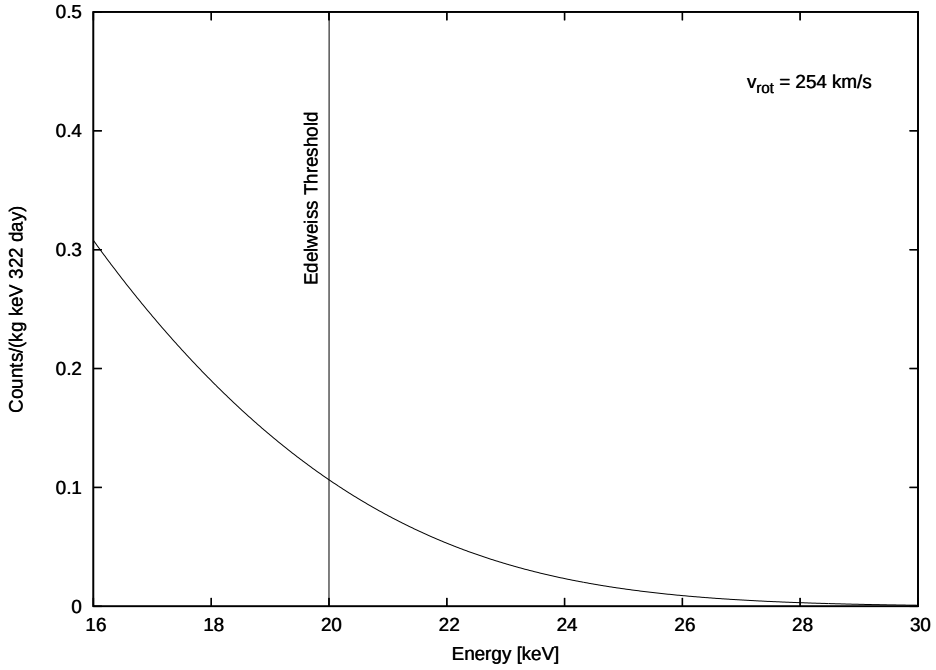

Figure 9b: Edelweiss spectrum for Fe' dark matter with $\epsilon\sqrt{\xi_{Fe'}} = 5.0 \times 10^{-11}$. We have assumed $v_{rot} = 254$ km/s.

The CDMS/Ge experiment finds two events at energies 12.3 and 15.5 keV which are clearly compatible with the shape of the predicted recoil energy spectrum for CDMS/Ge. Edelweiss finds 2 events in their acceptance region with energy just above threshold, which is also compatible with the shape of the predicted recoil energy spectrum for EdelweissII. It is therefore plausible that both of these experiments have detected Fe' dark matter. Under this assumption, we can obtain an estimate of the parameter: $\epsilon\sqrt{\xi_{Fe'}}$ for each of these experiments:

$$\begin{aligned} \epsilon\sqrt{Fe'} &= (3.5^{+2.8}_{-2.0}) \times 10^{-11} \text{ from CDMS/Ge} \\ \epsilon\sqrt{Fe'} &= (1.4^{+1.0}_{-0.8}) \times 10^{-10} \text{ from EdelweissII .} \end{aligned} \tag{42}$$

Here we have only included the statistical errors at 95% C.L. The systematic uncertainties can be quite large, given the rapidly rising event rates towards lower E_R. For example, we find that a 20% systematic uncertainty in energy scale would lead to a $\sim 20\%$ uncertainty in the estimate for $\epsilon\sqrt{\xi_{Fe'}}$ from CDMS/Ge and a 50% in the estimate for $\epsilon\sqrt{\xi_{Fe'}}$ from EdelweissII. Also note that the systematic uncertainties in the form factor begin to be quite significant for Edelweiss due to the large recoil energy threshold. Clearly systematic uncertainties can reconcile the two estimates of $\epsilon\sqrt{Fe'}$ from CDMS/Ge and EdelweissII. The XENON100 experiment, with an anticipated net exposure of over 1000 kg-days should be able to confirm the presence of a Fe' signal in the near future.

Combining the above estimate for $\epsilon\sqrt{\xi_{Fe'}}$ with our earlier fit for $\epsilon\sqrt{\xi_{A'}}$ suggests a $\xi_{Fe'}/\xi_{A'}$ fraction of around $\sim 10^{-2}$ which is plausible. Also note that such a small $\xi_{Fe'}$ component does not significantly affect the fit of the DAMA and CoGeNT experiments.

The CRESSTII experiment using a $CaWO_4$ target has recently reported 32 dark matter candidate events, with a background of around 9 events in their signal region, which suggests a statistically significant low energy excess of around 23 events. The threshold of CRESSTII is 10 keV_{nr}, with the excess of events reported in the oxygen band near threshold. The CRESSTII experiment is potentially sensitive to both the A' component and the Fe' component. We illustrate this in figure 10, where we give the predicted CRESST recoil energy spectrum for an example with parameters close to the DAMA/CoGeNT best fit. As this figure illustrates, the A' component is only important in the region near threshold, while the Fe' contribution is somewhat more spread out. Thus, in principle these two components can be distinguished from the observed energy distribution of events (so long as they both contribute significantly to the signal).

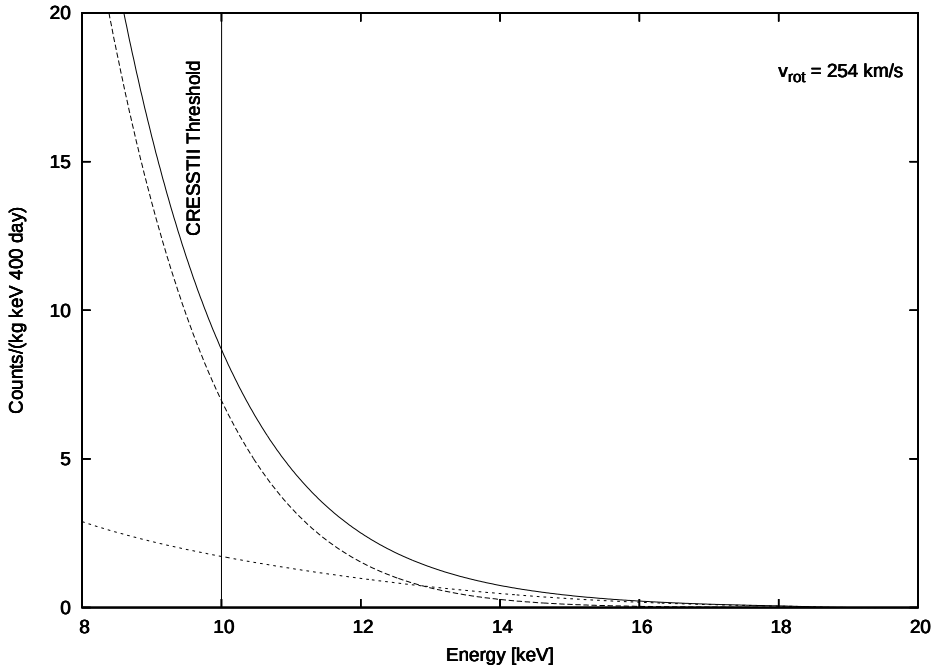

Figure 10: CRESSTII spectrum in the oxygen band for A', Fe' dark matter assuming $v_{rot} = 254$ km/s. The dashed line is the A' contribution with parameters $\epsilon\sqrt{\xi_{A'}} = 6 \times 10^{-10}$, $m_{A'} = 22.0$. The dotted line is for the Fe' contribution with parameters $\epsilon\sqrt{\xi_{Fe'}} = 1.0 \times 10^{-10}$. The solid line is the sum of the two contributions. [100% detection efficiency has been assumed, and a resolution of 0.3 keV].

We have found that the A' contribution has a very large annual modulation in the energy region above threshold. In fact,

$$\frac{\overline{dR}^1}{dE_R^m} \approx 0.5 \frac{\overline{dR}^0}{dE_R^m} \ . \tag{43}$$

The large annual modulation results because the interactions arise from A' particles in the tail of the narrow Maxwellian distribution and therefore can be greatly affected by small changes in the velocity of the Earth. Thus, if A' does contribute significantly to the signal, an examination of events in the $Ethreshold < E < Ethreshold + 3\ keV$ bin should show a statistically significant annual modulation with just 1-2 years of data. The annual modulation predicted for the Fe' events is smaller, but still quite large:

$$\frac{\overline{dR}^1}{dE_R^m} \approx 0.16 \frac{\overline{dR}^0}{dE_R^m} \tag{44}$$

and could also be eventually seen provided that a significant proportion of the events are due to Fe' interactions.

8 conclusion

In conclusion, we have confronted the mirror dark matter theory with the most recent experimental data. We examined the DAMA experiments allowing for the possibility of a negligible channeling fraction and showed that under that assumption the impressive DAMA signal can be fully explained. Mirror dark matter can simultaneously explain the CoGeNT low energy excess, and remains compatible with the results of the other experiments, including interesting hints of dark matter detection from CDMS/Ge, EdelweissII and CRESSTII. Taking into account some of the possible systematic uncertainties in quenching factor, detector resolution, galactic rotational velocity and velocity dispersion, we have mapped out the allowed regions of parameter space in the $m_{A'}, \epsilon\sqrt{\xi_{A'}}$ plane [Figures 4,5]. The net result is that the mirror dark matter candidate can explain all of the existing direct detection experiments, with parameters $\epsilon\sqrt{\xi_{A'}} = (7 \pm 3) \times 10^{-10}$, $m_{A'}/m_p = 22 \pm 8$, $\xi_{A'} \gtrsim 10^{-2}$, $\xi_{Fe'}/\xi_{A'} \sim 10^{-2}$.

Importantly this theory will soon be more stringently tested by: a) Further data from DAMA: in the near future the DAMA collaboration plan to upgrade their experiment with the aim of lowering their energy threshold. As illustrated in figure 1, they should see a change in sign of their modulation amplitude between 1.0-2.0 keVee. b) The CRESSTII experiment, with light target element O' and threshold 10 keV is potentially sensitive to both A' and Fe' components. They should find a rapidly falling energy spectrum with most of their events between 10 and 14 keV, with a very large annual modulation. c) The CDMS/Si experiment is sensitive to the dominant mirror metal component, A'. This experiment currently provides the

strongest constraint from the null experiments and limits $m_{A'}/m_p \stackrel{<}{\sim} 30$. Further data from CDMS/Si should either see a signal, or produce tighter constraints on $m_{A'}$. d) More data from the CoGeNT experiment should be helpful. Of particular note, is that mirror dark matter predicts a detectable annual modulation signal for CoGeNT (figure 6) with the distinctive feature that it changes in sign at energies around $E_R \approx 0.5 - 0.8$ keVee. e) Very sensitive but typically higher threshold experiments, such as CDMS/Ge, EdelweissII and XENON100 can potentially probe the heavier $\sim Fe'$ component which should exist at some level. The two events seen in CDMS/Ge and in EdelweissII are consistent with this component, and suggests $\xi_{Fe'}/\xi_{A'} \sim 10^{-2}$. f) In the longer term, directional experiments will be important due to the low velocity dispersion of mirror dark matter $[v_0[A'] \ll v_{rot}]$. [12]

Mirror dark matter is not expected to show up in collider experiments through the photon-mirror photon kinetic mixing induced interactions. However, the Higgs - mirror Higgs quartic interaction [Eq.(3)] leads to modifications of the properties of the Higgs boson[14] which can potentially be observed at the LHC and Tevatron[39]. Sensitive orthopositronium studies[40], might be able to directly probe $\epsilon \sim 10^{-9}$ and thus provide further tests of the mirror dark matter scenario. Such an experiment has been proposed recently in ref.[41].

Acknowledgments

This work was supported by the Australian Research Council.

References

[1] R. Bernabei *et al.* (DAMA Collaboration), Riv. Nuovo Cimento. 26, 1 (2003) [astro-ph/0307403]; Int. J. Mod. Phys. D13, 2127 (2004); Phys. Lett. B480, 23 (2000).

[2] R. Bernabei *et al.* (DAMA Collaboration), Eur. Phys. J. C56: 333 (2008) [arXiv:0804.2741].

[3] R. Bernabei *et al.* (DAMA Collaboration), arXiv: 1002.1028.

[4] C. E. Aalseth *et al.* (CoGeNT Collaboration), arXiv:1002.4703.

[5] Z. Ahmed *et al.* (CDMS Collaboration), arXiv: 0912.3592.

[6] Z. Ahmed *et al.* (CDMS Collaboration), Phys. Rev. D81: 042002 (2010) [arXiv: 0907.1438].

[7] W. Seidel (for the CRESST collaboration), Talk given at IDM2010, July 2010.

[12] A dark matter detection experiment in the southern hemisphere would be very useful because, due to the Earth's orientation, it could sensitively probe the possible diurnal variation if there are accumulated mirror particles in the Earth's core.

[8] E. Armengaud (for the Edelweiss Collaboration), Talk given at IDM2010, July 2010; Phys. Lett. B687, 294 (2010) [arXiv:0912.0805].

[9] R. Foot, Phys. Rev. D69, 036001 (2004) [hep-ph/0308254]; Mod. Phys. Lett. A19, 1841 (2004) [astro-ph/0405362]; Phys. Rev. D74, 023514 (2006) [astro-ph/0510705].

[10] R. Foot, Phys. Rev. D78, 043529 (2008) [arXiv: 0804.4518].

[11] R. Foot, Phys. Rev. D80, 091701 (2009) [arXiv:0909.3126].

[12] R. Foot, Phys. Rev. D81, 087302 (2010) [arXiv:1001.0096].

[13] R. Foot, arXiv:1004.1424.

[14] R. Foot, H. Lew and R. R. Volkas, Phys. Lett. B272, 67 (1991); Mod. Phys. Lett. A7, 2567 (1992).

[15] R. Foot, Int. J. Mod. Phys. D13, 2161 (2004) [astro-ph/0407623].

[16] R. Foot and R. R. Volkas, Phys. Rev. D70, 123508 (2004) [astro-ph/0407522].

[17] R. Foot and X-G. He, Phys. Lett. B267, 509 (1991).

[18] T. D. Lee and C. N. Yang, Phys. Rev. 104, 256 (1956); I. Kobzarev, L. Okun and I. Pommeranchuk, Sov. J. Nucl. Phys. 3, 837 (1966); M. Pavsic, Int. J. Theor. Phys. 9, 229 (1974).

[19] C. Alcock *et al.* (MACHO collaboration), ApJ, 542, 281 (2000) [arXiv: astro-ph/0001272]; P. Tisserand *et al.*, (EROS Collaboration) Astron. Astrophys, 469, 387 (2007) [arXiv: astro-ph/0607207].

[20] D. Clowe *et al.*, Astrophys. J. 648, L109 (2006) [astro-ph/0608407].

[21] Z. K. Silagadze, arXiv:0808.2595.

[22] R. Foot, A. Yu. Ignatiev and R. R. Volkas, Phys. Lett. B503, 355 (2001) [arXiv: astro-ph/0011156]; R. Foot, Int. J. Mod. Phys. A19 3807 (2004) [astro-ph/0309330]; R. Foot and Z. K. Silagadze, Int. J. Mod. Phys. D14, 143 (2005) [astro-ph/0404515]; P. Ciarcelluti and R. Foot, Phys. Lett. B679, 278 (2009) [arXiv: 0809.4438]. See also, S. Davidson, S. Hannestad and G. Raffelt, JHEP 5, 3 (2000) [arXiv: hep-ph/0001179].

[23] G. Raffelt, *Stars as Laboratories for Fundamental Physics,* Chicago University Press (1996).

[24] P. Ciarcelluti and R. Foot, Phys. Lett. B690, 462 (2010) [arXiv:1003.0880].

[25] Z. Berezhiani *et al.*, Astropart. Phys. 24, 495 (2006) [astro-ph/0507153].

[26] Z. Berezhiani, D. Comelli and F. L. Villante, Phys. Lett. B503, 362 (2001) [hep-ph/0008105]; L. Bento and Z. Berezhiani, Phys. Rev. Lett. 87, 231304 (2001) [hep-ph/0107281]; A. Yu. Ignatiev and R. R. Volkas, Phys. Rev. D68, 023518 (2003) [hep-ph/0304260]; R. Foot and R. R. Volkas, Phys. Rev. D68, 021304 (2003) [hep-ph/0304261]; Phys. Rev. D69, 123510 (2004) [hep-ph/0402267]; Z. Berezhiani, P. Ciarcelluti, D. Comelli and F. L. Villante, Int. J. Mod. Phys. D14, 107 (2005) [astro-ph/0312605]; P. Ciarcelluti, Int. J. Mod. Phys. D14, 187 (2005) [astro-ph/0409630]; Int. J. Mod. Phys. D14, 223 (2005) [astro-ph/0409633].

[27] R. H, Helm, Phys. Rev. 104, 1466 (1956).

[28] J. D. Lewin and P. F. Smith, Astropart. Phys. 6, 87 (1996).

[29] M. J. Reid *et al.*, Astrophys. J. 700, 137 (2009) [arXiv: 0902.3913].

[30] A. K. Drukier, K. Freese and D. N. Spergel, Phys. Rev. D33, 3495 (1986); K. Freese, J. A. Frieman and A. Gould, Phys. Rev. D37, 3388 (1988).

[31] R. Bernabei *et al.* (DAMA Collaboration), Nucl. Instrum. Meth. A592: 297 (2008) [arXiv: 0804.2738].

[32] N. Bozorgnia, G.B. Gelmini and P. Gondolo, arXiv: 1006.3110.

[33] R. Bernabei *et al.* (DAMA Collaboration), Eur. Phys. J. C53, 205 (2008) [arXiv: 0710.0288].

[34] D. Hooper, J. I. Collar, J. Hall and D. McKinsey, arXiv: 1007.1005.

[35] C. E. Aalseth *et al.* (CoGeNT Collaboration), Phys. Rev. Lett. 101, 251301 (2008) [arXiv: 0807.0879].

[36] J. P. Filippini, Ph.D thesis, 2008.

[37] E. Aprile *et al.* (XENON100 Collaboration), arXiv: 1005.0380 (2010).

[38] J. I. Collar and D. N. McKinsey, arXiv:1005.0838; arXiv: 1005.3723; The Xenon Collaboration, arXiv: 1005.2615; J. I. Collar, arXiv: 1006.2031; P. Sorensen, arXiv: 1007.3549.

[39] A. Yu. Ignatiev and R. R. Volkas, Phys. Lett. B487, 294 (2000) [hep-ph/0005238]; R. Barbieri, T. Gregoire and L. J. Hall, hep-ph/0509242; W. Li, P. Yin and S. Zhu, Phys. Rev. D76, 095012 (2007) [arXiv: 0709.1586].

[40] S. L. Glashow, Phys. Lett. B167, 35 (1986); R. Foot and S. N. Gninenko, Phys. Lett. B480, 171 (2000) [hep-ph/0003278].

[41] P. Crivelli *et al.*, arXiv: 1005.4802.